Tsunami Hazard Associated with Makran Subduction Zone along the Southern Coasts of Iran

Mohammad Heidarzadeh
PhD Candidate of Civil Engineering, College of Eng., University of Tehran, Tehran, Iran
Email: mohammad_heidarzadeh@yahoo.com, Tel: 0911 113 4123, Fax: 021-22222407
Moharram Dolatshahi Pirooz
Assistant professor of Civil Engineering, College of Eng., University of Tehran, Tehran, Iran
Nasser Hajizadeh Zaker
Assistant professor of Environmental Engineering, University of Tehran, Tehran, Iran
Mohammad Mokhtari
Assistant professor, International Institute of Earthquake Engineering and Seismology, Tehran, Iran

Abstract:
In this paper the tsunami hazard associated with Makran subduction zone along the southern coasts of Iran is investigated. Several harbors and ports lie in southern coasts of Iran in the vicinity of Indian Ocean. Disruption of operations at these ports due to tsunami waves could impact the national and also regional economies. Therefore, it is necessary to investigate the hazard of tsunami and its possible impacts on coastal structures. The Makran subduction zone is among two main tsunamigenic zones in the Indian Ocean. In this zone the Oman oceanic plate subducts beneath the Iranian Microplate at an estimated rate of about 19 mm/yr. Historically, there is the potential for tsunami generation in this region and several tsunamis attacked the Makran coastlines in the past. The most recent tsunami in this region has occurred on 28 November 1945 which took the lives of more than 4000 people in the coasts of Iran, Pakistan, India, and Oman. Here we examine the seafloor uplift of the Makran zone and its potential for generating destructive tsunamis in the southern coastlines of Iran. Several earthquake scenarios with moment magnitudes ranging between 6.0 and 8.5 are used as initial conditions for analysis. The epicenter of the 1945 event is used as the epicenter for different tsunami scenarios in this study. For each scenario the propagation of tsunami waves on coastlines is calculated, which is the key parameter for tsunami hazard assessment and harbor protection.

Introduction:

The December 2004 Indian Ocean tsunami has brought the need to assess tsunami hazards in various parts of the world, especially in the Indian Ocean basin to the attention of the international community. This megatsunami underscored the extraordinary social and economic damage that such an event can bring. Also, it showed that the risk of tsunami is real for the Indian Ocean basin and it is necessary to take appropriate measures to protect people living in coastal regions of this ocean.

Researchers working in the field of tsunami modeling have long known that the main source for nearly all tsunami-producing earthquakes is subduction zones [1]. Two main subduction zones that can trigger tsunami generating earthquakes in the Indian Ocean basin include the Indonesian subduction zone in the east and the Makran subduction zone in the north (Figure 1) [2]. The Indonesian subduction zone has produced three large earthquakes followed by devastating tsunami waves in the recent two years. These earthquakes and associated tsunamis include the 26 December 2004 tragedy, the 28 March 2005, and 17 July 2006 events in the Indian Ocean which took the lives of about 225000, 1000, and 401 people in coastal zones on this ocean respectively [1&3].

The other important tsunamigenic zone in the Indian Ocean basin is Makran subduction zone (MSZ) located off the southern coasts of Iran and Pakistan in the north-western Indian Ocean. As can be seen from figure 1, Makran possible tsunami has the potential to affect Iran, Oman, Pakistan, and India. In this region the Oman oceanic lithosphere slips below the Iranian micro-plate at the estimated rate of about 19 mm/yr [4]. The last major historical earthquake and tsunami in the MSZ occurred on 28 November 1945 at 21:56 local time. The epicenter of the earthquake was located at latitude 24.50 ºN and

longitude 63.00 ºE, about 87.1 kilometers from the south west of Churi, Pakistan. The magnitude of the earthquake was evaluated to be 8.1 [5&6]. In fact, this was the last major tsunami-generating earthquake in the Makran zone. The destructive tsunami killed more than 4,000 people and caused great loss of life and devastation along the coasts of Western India, Iran, Oman and Pakistan [5&6&7]. Based on the above-mentioned facts, the risk of tsunami in southern coasts of Iran bordering the Indian Ocean is relatively high and it is necessary to investigate the hazard of tsunami and take appropriate preparedness and mitigation measures. Although tsunami can not be prevented, its destructive consequences such as loss of life and property can be reduced by taking convenient planning. To plan for the tsunami hazard, having a good understanding of tsunami is inevitable. In this order the generation mechanism of tsunami, the propagation of tsunami waves and finally its wave height in coastlines are of vital importance for tsunami hazard assessment and these parameters should be understood and calculated carefully. Hence, in this paper to assess the tsunami hazard associated with Makran zone, the modeling of tsunami is performed. Based on the tsunami modeling the key parameters such as the extent of seafloor deformation due to earthquake occurrence, tsunami travel time to the coastlines, the pattern of wave propagation, and the runup on shorelines can be estimated. The mentioned parameters can be used to develop inundation map, evacuation map, and finally to develop a tsunami warning system for the Iranian southern vulnerable coastlines. In the following sections of this paper, at first the modeling of tsunami generation will be discussed and then the propagation of possible tsunami in MSZ will be presented.

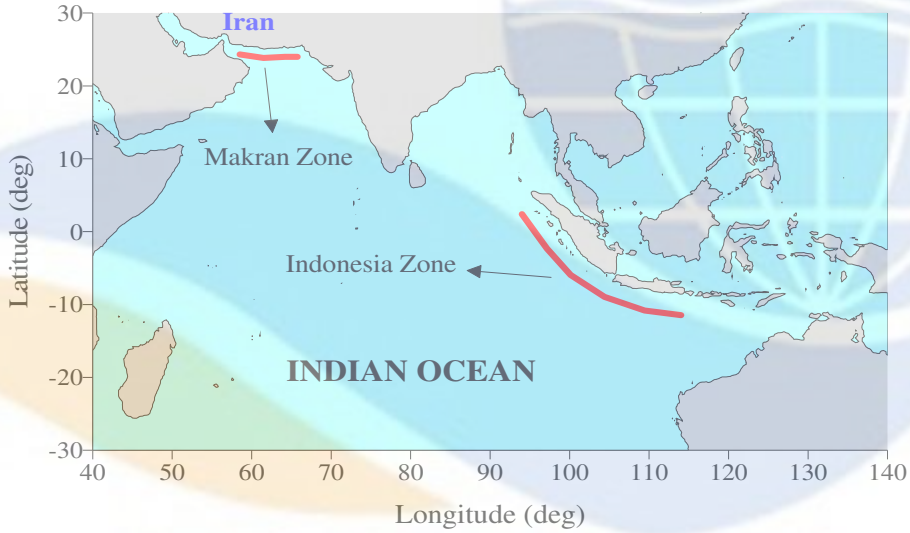

Figure (1): Two tsunamigenic sources in the Indian Ocean

Modeling of Tsunami Generation in the MSZ:

The deformation of ocean floor is responsible for tsunami generation. After the earthquake occurrence the earth's crust experiences vertical movement in the form of uplift and subsidence at the location of subduction zone. The resulted seafloor deformation provides the initial condition for the tsunami propagation and runup modeling [8]. Several earthquake scenarios with moment magnitudes ranging between 6.5 and 8.5 are used as initial conditions for analysis. The epicenter of the different tsunami scenarios are placed at latitude 24.50 ºN and longitude 63.00 ºE in this study.

Earthquakes typically have rupture durations of minutes, which can be considered as instantaneous when compared to the time scale of the subsequent tsunamis. Kajiura (1970) suggested that for tsunami modeling the initial surface wave can be assumed as identical to the vertical component of the seafloor deformation due to faulting [9]. Here, the algorithm of Mansinha and Smylie (1971) is used to calculate the seafloor deformation based on input seismic parameters that include the strike, dip, and slip angles, the amount of slip, and the dimensions and location of the fault. In this study, empirical relations presented by Wells and Coppersmith (1994) [10] are used to related the moment magnitude of the underwater earthquake to the fault parameters (equations 1 to 3).

$$Log(u) = -4.80 + 0.69M \quad (1)$$

$$Log(L) = -3.22 + 0.69M \quad (2)$$

$$Log(W) = -1.01 + 0.32M \quad (3)$$

where u is the displacement on the fault surface, L and W are fault length and width respectively and M is the earthquake magnitude. Table 1 summarizes the fault parameters used in this study for MSZ. The results of tsunami generation analysis for different earthquake scenarios are presented in Table 2. Columns 5 and 6 of Table 2 show the maximum uplift and subsidence of the ocean floor in the location of Makran subduction zone due to earthquake occurrence. A two dimensional views of the seafloor deformation is presented in figure 2 for the case of magnitude 8.1 earthquake. Figure 3 shows the pattern and extent of deformation for various scenarios. As can be seen, for earthquake scenarios with magnitude greater than 7.5 the maximum seafloor uplift is considerable indicating high possibility for tsunami generation. In this order, it is useful to consider the fact that for near-field events like Makran tsunamis, the maximum wave runup can be estimated as two times the maximum seafloor displacement [11].

Table (1): Fault parameters used for tsunami source analysis

Displacement (deg)	Length (km)	Width (km)	Dip Angle (deg)	Strike Angle (deg)	Slip Angle (deg)	Depth (km)
Equ. (1)	Equ. (2)	Equ. (3)	10	270	100	20

Table (2): Results of tsunami generation analysis

Earthquake Magnitude	Rapture Length (km)	Rapture Width (km)	Displacement (m)	Maximum Uplift (m)	Maximum subsidence (m)
6.5	18	12	0.48	+0.03	-0.02
6.8	30	15	0.78	+0.09	-0.05
7.0	41	17	1.10	+0.17	-0.09
7.3	66	21	1.70	+0.34	-0.20
7.5	92	25	2.40	+0.55	-0.33
7.7	124	28	3.30	+0.80	-0.50
7.8	145	31	3.80	+1.00	-0.60
8.0	200	35	5.20	+1.46	-0.87
8.1	234	38	6.20	+1.80	-1.10
8.2	274	41	7.20	+2.16	-1.30
8.3	321	44	8.50	+2.61	-1.57
8.4	376	48	9.90	+3.13	-1.89
8.5	442	51	11.6	+3.70	-2.30

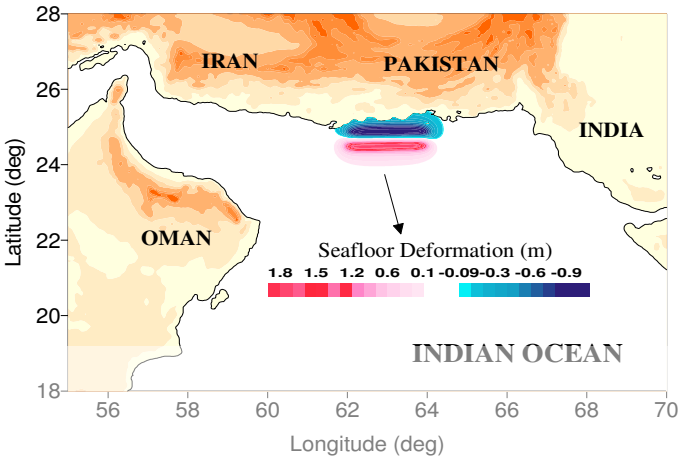

Figure (2): 2D seafloor deformation for M 8.1 earthquake

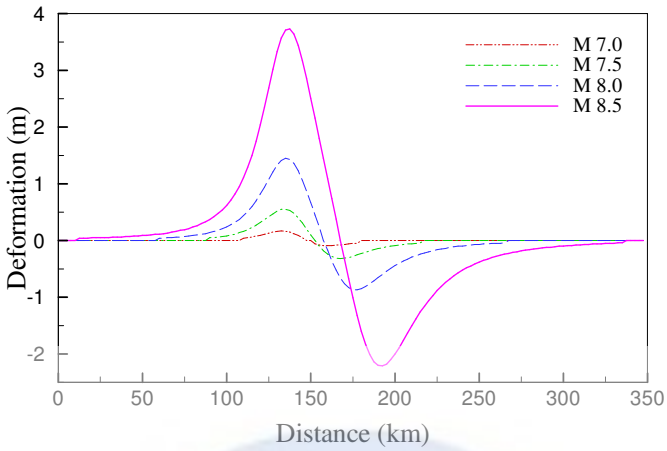

Figure (3): Seafloor deformation for various scenarios

Modeling of Tsunami Propagation in the MSZ:

Since tsunami wavelengths (hundred of kilometers) are much larger than the ocean depth (a few kilometers), tsunamis are considered as shallow water waves, following the long wave theory. In the long wave theory the vertical acceleration of water particles is negligible compared to the gravitational acceleration, and the hydrostatic pressure approximation is used. It may be added that under the assumption of long wave theory, the hydrodynamic equations describing the conservation of mass (equation 4) and momentum (equation 5) can be depth averaged [11].

$$\frac{\partial(\eta+h)}{\partial t}+\nabla[v(\eta+h)]=0 \quad (4)$$

$$\frac{\partial v}{\partial t}+(v\nabla)v=-g\nabla\eta+\sum f \quad (5)$$

where h is the sea depth and η the water elevation above mean sea level, v is the depth-averaged horizontal velocity vector, g is the gravity acceleration, and f represents bottom friction and Coriolis forces. The above system is completed by suitable boundary conditions that are of pure wave reflection on the solid boundary and of full wave transmission on the open sea:

$v.n=2(c_1-c_0)$ on the open sea (6)

$v.n=0$ on the solid boundary (7)

where $c_0=\sqrt{gh}$ is the phase velocity of the linear wave and $c_1=\sqrt{g(h+\eta)}$ is the local phase velocity (non-linear waves). Due to close distance of about 150 km between the Makran subduction zone and Iranian coastal regions, there is the threat of near-field tsunamis in southern coasts of Iran. In the case of near-field tsunamis, that is, those whose propagation distance is less than 1000 km, the model of plane Earth with no rotation is applied and the Cartesian coordinates can be used. In other words, the coriolis forces and the Earth's curvature can be neglected. Based on these approximations, for near-field tsunami propagation the vertically integrated governing equations are in the following form [12].

$$\frac{\partial\eta}{\partial t}+\frac{\partial M}{\partial x}+\frac{\partial N}{\partial y}=0 \quad (8)$$

$$\frac{\partial M}{\partial t}+\frac{\partial}{\partial x}\left(\frac{M^2}{D}\right)+\frac{\partial}{\partial y}\left(\frac{MN}{D}\right)+gD\frac{\partial\eta}{\partial x}+\tau_x D=0 \quad (9)$$

$$\frac{\partial N}{\partial t}+\frac{\partial}{\partial x}\left(\frac{MN}{D}\right)+\frac{\partial}{\partial y}\left(\frac{N^2}{D}\right)+gD\frac{\partial \eta}{\partial y}+\tau_y D=0 \quad (10)$$

Where, $M=U(h+\eta)=UD$, $N=V(h+\eta)=VD$, $\tau_x=\frac{gn^2}{D^{10/3}}M\sqrt{M^2+N^2}$, $\tau_y=\frac{gn^2}{D^{10/3}}N\sqrt{M^2+N^2}$

(M, N) are the horizontal components of the discharge per unit width, (U, V) are the vertically averaged horizontal particle velocities, g is the gravitational acceleration, h is still water depth, η the vertical displacement of the water surface above the still water level (z = 0), D is the total water depth $(h+\eta)$, n is Manning's roughness coefficient, and τ_x and τ_y are bottom frictional terms in x and y directions, respectively. In this study, the governing equations are solved by the finite difference technique with leap-frog scheme. The bathymetry of the Makran region was obtained from the British Oceanographic Data Center with 2000 m grid size. The time step is selected as 1 s to satisfy the stability condition. The total number of grid points in the study area is 224450 (670 × 335). Along the depth of 20 m contour line the vertical wall boundary condition is assumed. Considering Table 2, the tsunami propagation modeling is performed for the case of magnitude 8.1 earthquake. In our study, waveform and height can be predicted at any location in the calculation area. To facilitate wave height prediction, a number of reference locations are selected to record time histories of tsunami waves. The longitude and latitude of the selected reference locations are listed in Table 3. In addition, figure 4 shows the calculation area along with the reference locations. Figures 5, 6 and 7 present time histories of wave height in the shown reference locations. Figures 8 and 9 show snapshots of the water surface at times t = 5, and 10 minutes.

Table (3): Longitude and latitude of the selected reference locations

Location No.	Country Name	Site Name	Longitude (deg)	Latitude (deg)
1	IRAN	Jask	57.76	25.62
2		Kereti	59.09	25.34
3		Kalak	59.37	25.29
4		Bir	59.81	25.32
5		Gurdim	60.12	25.29
6		Chabahar	60.60	25.22
7		Beris	61.17	25.05
8	PAKISTAN	Jwani	61.75	24.92
9		Gwadar	62.33	25.02
10		Pasni	63.49	25.06
11		Ormara	64.64	25.08
12	OMAN	Suhar	56.83	24.36
13		Mascat	58.65	23.64
14		Sur	59.54	22.64

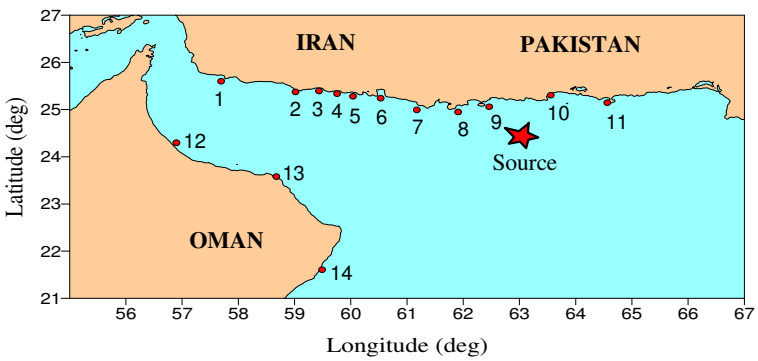

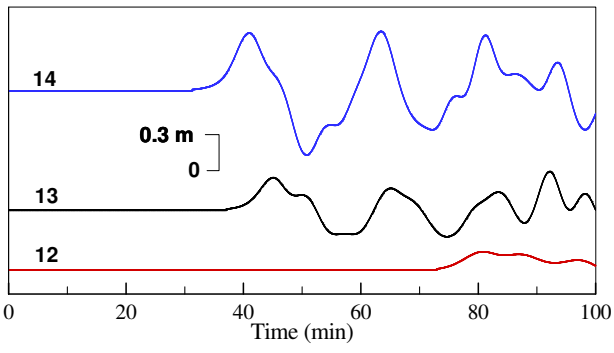

Figure (4): Calculation area along with the reference locations

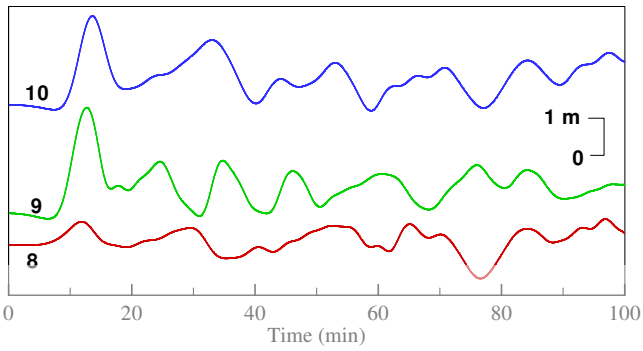

Figure (5): Wave height time history for Oman

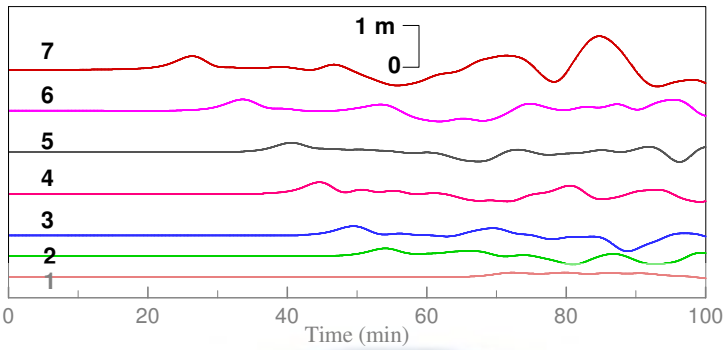

Figure (6): Wave height time history for Iran coastlines

Figure (7): Wave height time history for Pakistan coasts

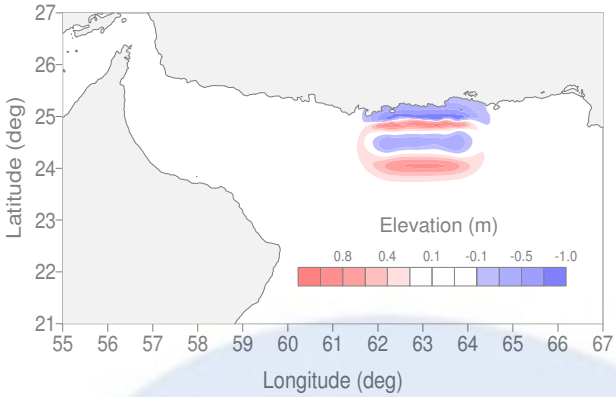

Figure (8): Snapshot at times t = 5 minutes

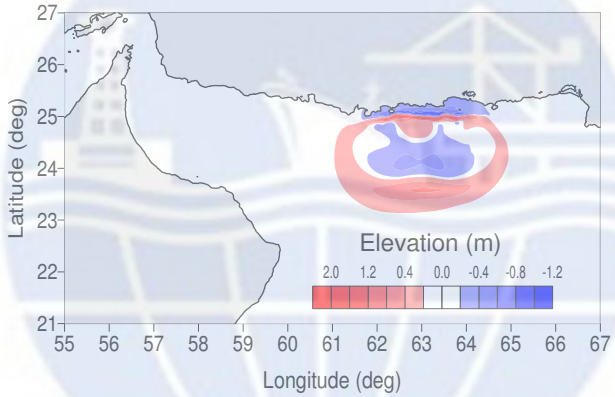

Figure (9): Snapshot at times t = 10 minutes

Discussion and Conclusion:

Numerical simulations of tsunami generation and propagation are presented to examine probable tsunami originating from the Makran subduction zone of the North Indian Ocean. Tsunami generation modeling shows that for earthquake scenarios with magnitude greater than 7.5 the maximum seafloor uplift is considerable indicating high possibility for tsunami generation. A numerical model based on finite difference technique with leap-frog scheme was employed to model tsunami propagation. Using this model the waveform and height time histories in the selected reference locations are presented. The propagation modeling was performed only for the case of magnitude 8.1 earthquake at the at latitude 24.50 ºN and longitude 63.00 ºE. In this case as can be seen from figure 7, first tsunami waves hit the Iranian coastlines after about 20 minutes. It is obvious that by moving the earthquake epicenter to the west of the MSZ, the travel time will decrease. Also, figure 7 shows that for the investigated tsunami source, the tsunami wave height in some parts of the Iranian southern coastlines is considerable. For example, in the reference site number 7 the wave height is about 70 cm. The results of this study can be used to develop inundation and evacuation map as well as to develop a tsunami warning system for Iranian vulnerable coastlines. To do so, similar simulations should be performed considering different tsunami source scenarios. For each tsunami source scenario, the tsunami wave characteristics including travel time, propagation and runup are calculated and the inundation and evacuation map will be constructed based on worst case scenarios.

References:

[1]. Geist E. L., Titov V. V. and Synolakis C. E., (2006), "Tsunami: Wave of Change", Scientific American, January 2006, pp 56-63

[2]. International Oceanographic Commission (IOC), (2005), "Intergovernmental Coordination Group for the Indian Ocean Tsunami Warning and Mitigation System (ICG/IOTWS) ", Reports of Governing and Major Subsidiary Bodies , First Session, 3-5 August, Perth, Western Australia

[3]. http://earthquake.usgs.gov
[4]. Vernant Ph. et al., (2004), "Present-Day Crustal Deformation and Plate Kinematics in the Middle East Constrained by GPS Measurements in Iran and Northern Oman", Geophys. J. Int., Vol. 157, pp 381-398
[5]. Mokhtari, M., Farahbod, A.M., (2005), "Tsunami Occurrence in the Makran Region", Tsunami Seminar, 26th February, Tehran, Iran
[6]. Carayannis G. P., (2004), "The Earthquake and Tsunami of 28 November 1945 in Southern Pakistan", International Conference HAZARDS 2004, 2-4 Dec., Hyderabad, India
[7]. Ambraseys N. N. and Melville C. P., (1982), "A History of Persian Earthquakes", Cambridge University Press, Britain
[8]. Legg M. R., Eeri M., Borrero J. C., and Synolakis C. E., (2004), "Tsunami Hazard Associated With Catalina Fault in Southern California", Earthquake Spectra, Vol. 20, No. 3, pp 1–34, August 2004, Earthquake Engineering Research Institute
[9]. Weil Y., Cheung K. F., Curtis G. D., and McCreery C. S. (2003), "Inverse Algorithm for Tsunami Forecasts", J. of Waterway, Port, Coastal and Ocean Eng., ASCE, March/April
[10]. Wells D. L. and Coppersmith K. J., (1994), "New Empirical Relationships among Magnitude, Rupture Length, Rupture Width, Rupture Area, and Surface Displacement", Bulletin of the Seismological Society of America, Vol. 84, No. 4, pp. 974-1002
[11]. Synolakis, C. E., (2003), "Tsunami and Seiche", CRC Press, Boca Raton, Florida, USA
[12]. Zahibo N., Pelinovsky E., Talipova T., Kozelkov A., Kurkin A., (2005), "Analytical and Numerical Study of Nonlinear effects at Tsunami Modeling", Applied Mathematics and Computation, 174 (2006) 795–809